We are IntechOpen,
the world's leading publisher of
Open Access books
Built by scientists, for scientists

6,900
Open access books available

185,000
International authors and editors

200M
Downloads

Our authors are among the

154
Countries delivered to

TOP 1%
most cited scientists

12.2%
Contributors from top 500 universities

CLARIVATE ANALYTICS
BOOK CITATION INDEX
INDEXED

WEB OF SCIENCE™

Selection of our books indexed in the Book Citation Index
in Web of Science™ Core Collection (BKCI)

Interested in publishing with us?
Contact book.department@intechopen.com

Numbers displayed above are based on latest data collected.
For more information visit www.intechopen.com

5

3D Coalescence Collision of Liquid Drops Using Smoothed Particle Hydrodynamics

Alejandro Acevedo-Malavé and Máximo García-Sucre
Venezuelan Institute for Scientific Research (IVIC)
Venezuela

1. Introduction

The importance of modeling liquid drops collisions (see figure 1) is due to the existence of natural and engineering process where it is useful to understand the droplets dynamics in specific phenomena. Examples of applications are the combustion of fuel sprays, spray coating, emulsification, waste treatment and raindrop formation (Bozzano & Dente, 2010; Bradley & Stow, 1978;Park & Blair, 1975; Rourke & Bracco, 1980; Shah et al., 1972).

In this study we apply the Smoothed Particle Hydrodynamics method (SPH) to simulate for the first time the hydrodynamic collision of liquid drops on a vacuum environment in a three-dimensional space. When two drops collide a circular flat film is formed, and for sufficiently energetic collisions the evolution of the dynamics leads to a broken interface and to a bigger drop as a result of coalescence. We have shown that the SPH method can be useful to simulate in 3D this kind of process. As a result of the collision between the droplets the formation of a circular flat film is observed and depending on the approach velocity between the droplets different scenarios may arise: (i) if the film formed on the droplets collision is stable, then flocks of attached drops can appear; (ii) if the attractive interaction across the interfacial film is predominant, then the film is unstable and ruptures may occur leading to the formation of a bigger drop (permanent coalescence); (iii) under certain conditions the drops can rebound and the emulsion will be stable. Another possible scenario when two drops collide in a vacuum environment is the fragmentation of the drops.

Many studies has been proposed for the numerical simulation of the coalescence and break up of droplets (Azizi & Al Taweel, 2010; Cristini et al., 2001; Decent et al., 2006; Eggers et al., 1999; Foote ,1974; Jia et al., 2006; Mashayek et al., 2003; Narsimhan, 2004; Nobari et al., 1996; Pan & Suga, 2005; Roisman, 2004; Roisman et al., 2009; Sun et al., 2009; Xing et al., 2007; Yoon et al., 2007). In these studies, the authors propose different methods to approach the dynamics of liquid drops by a numerical integration of the Navier-Stokes equations. These examine the motion of droplets and the dynamics that it follows in time and study the liquid bridge that arises when two drops collide. The effects of parameters such as Reynolds number, impact velocity, drop size ratio and internal circulation are investigated and different regimes for droplets collisions are simulated. In some cases, those calculations yield results corresponding to four regimes of binary collisions: bouncing, coalescence, reflexive separation and stretching separation. These numerical simulations suggest that the collisions that lead to rebound between the drops are governed by macroscopic dynamics. In these simulations the mechanism of formation of satellite drops was also studied,

confirming that the principal cause of the formation of satellite drops is the "end pinching" while the capillary wave instabilities are the dominant feature in cases where a large value of the parameter impact is employed.

Experimental studies on the coalescence process involving the production of satellite droplets has been reported in the literature (Ashgriz & Givi, 1987, 1989; Brenn & Frohn, 1989; Brenn & Kolobaric, 2006; Zhang et al., 2009). These authors found out that when the Weber number increases, the collision takes the form of a high-energy one and results of different type may arise. In these references the results show that the collision of the droplets can be bouncing, grazing and generating satellite drops. Based on data from experiments on the formation and breaking up of ligaments, the process of satellite droplets formation is modeled by these authors and the experiments are carried out using various liquid streams. On the other hand, for Weber numbers corresponding to a high-energy collision, permanent coalescence occurs and the bigger drop is deformed producing satellite drops. Experimental studies on the binary collision of droplets for a wide range of Weber numbers and impact parameters have been carried out and reported in the literature (Ashgriz & Poo, 1990; Gotaas et al., 2007b; Menchaca-Rocha et al., 1997; Qian & Law, 1997). These authors identified two types of collisions leading to drops separation, which can be reflexive or stretching separation. It was found that the reflexive separation occurs for head-on collisions, while stretching separation occurs for high values of the impact parameter. Carrying out Experiments, the authors reported the transition between two types of separation, and also collisions that lead to coalescence. In these references experimental investigations of the transition between different regimes of collisions were reported. The authors analyzed the results using photographic images, which showed the evolution of the dynamics exhibited by the droplets. As a result of these experiments were proposed five different regimes governing the collision between droplets: (i) coalescence after a small deformation, (ii) bouncing, (iii) coalescence after substantial deformation, (iv) coalescence followed by separation for head-on collisions, and (v) coalescence followed by separation for off-center collisions.

Li (1994) and Chen (1985) studied the coalescence of two small bubbles or drops using a model for the dynamics of the thinning film in which both, London-van der Waals and electrostatic double layer forces, are taken into account. Li (1994) proposes a general expression for the coalescence time in the absence of the electrostatic double layer forces. The model proposed by Chen (1985), depending on radius of the drops and the physical properties of the fluids and surfaces, describes the film profile evolution and predicts the film stability, time scale and film thickness.

The dynamics of collision between equal-sized liquid drops of organic substances has also been reported in the literature (Ashgriz & Givi, 1987, 1989; Gotaas et al., 2007a; Jiang et al., 1992; Podgorska, 2007). They reported the experimental results of the collision of water and normal-alkane droplets in the radius range of 150 μm. These results showed that for the studied range of Weber numbers, the behavior of hydrocarbon droplets is more complex than the observed for water droplets. For water droplets head-on collisions, permanent coalescence always result. Experimental studies on the different ways in which may occur the coalescence of drops, have been performed by different authors (Gokhale et al., 2004; Leal, 2004; Menchaca-Rocha et al., 2001; Mohamed-Kassim & Longmire, 2004; Thoroddsen et al., 2007; Wang et al., 2009; Wu et al., 2004). In these studies are reported the evolution in time of the surface shape as well as a broad view of the contact region between the droplets.

Tartakovsky & Meakin (2005) have shown that the artificial surface tension that emerge from the standard formulation of the Smoothed Particle Hydrodynamics (SPH) method (Gingold & Monaghan, 1977) could be eliminated by using SPH equations based on the number density of particles instead of the density of particles in the fluid. The contribution of Tartakovsky & Meakin (2005) could be very useful when modeling the hydrodynamic interaction of drops in liquid emulsions. Combining these schemes with some continuous-discrete hybrid approach (Cui et al., 2006; Koumoutsakos, 2005; Li et al., 1998; Nie et al., 2004; O'Connell & Thompson, 1995) it could be constructed an interesting model to discuss the collapse and disappearance of the interfacial film in emulsion media (Bibette et al., 1992; Ivanov & Dimitrov, 1988; Ivanov & Kralchevsky, 1997; Kabalnov & Wennerström, 1996; Sharma & Ruckenstein, 1987). Ivanov & Kralchevsky (1997) conducted a study on the possible outcomes for the collision of liquid droplets in emulsions. According to this study, when the collision between two drops occurs, an interfacial film of flat circular section is formed, and coalescence or flocculation may arise (Ivanov & Kralchevsky, 1997). These authors did not carry out the hydrodynamical modeling of collision between drops. Instead, they discuss thermodynamics and hydrodynamics aspects of the problem and raise some possible outcomes when two liquid droplets collide.

In this work we apply the SPH method to simulate for the first time in three-dimensional space the hydrodynamic coalescence collision of liquid drops in a vacuum environment. This method is employed in order to obtaining approximate numerical solutions of the equations of fluid dynamics by replacing the fluid with a set of particles. These particles may be interpreted as corresponding to interpolation points from which properties of the fluid can be determined. Each SPH particle can be considered as a system of smaller particles. The SPH method is particularly useful when the fluid motion produce big deformations and a large velocity of the whole fluid.

All our calculations were performed defining inside the SPH code two drops composed by 4700 SPH particles, running on a Dell Work Station with 8 processors Intel Xeon of 3.33 Ghz with 32.0 GB of RAM memory.

2. Smoothed particle hydrodynamics method

The SPH method was invented first and simultaneously by Lucy, (1977) and Gingold & Monaghan (1977) to solve astrophysical problems. This method has been used to study a range of astrophysical topics including formation of galaxies, formation of stars, supernovas, stellar collisions, and so on. This method has the advantage that if you want to model more than one material, the interface problems arising can be modeled easily, while they are hard to model using other methods based on finite differences. An additional advantage is that SPH method can be considered as a bridge between continuous and fragmented material, which makes it one of the best method to study problems of fragmentation in solids (Benz & Asphaug, 1994, 1995). Another feature that makes the SPH method attractive is that it yields solutions depending on space and time, making it versatile for treating a wide variety of problems in physics. Furthermore, given the similarity between SPH and molecular dynamics, combination of these two methods can be used to treat complex problems in systems that differ considerably in their length scales. The easiness of the method to be adaptable and their Lagrangian character make of SPH one of the most popular among existing numerical methods used for modeling fluids. On the other hand, the SPH method can be used to describe the dynamics of deformable bodies (Desbrun

& Gascuel, 1996). Currently there are several applications of SPH in different areas related to fluid dynamics, such as: incompressible flows, elastic flows, multiphase flows, supersonic flows, shock wave simulation, heat transfer, explosive phenomena, and so on (Liu & Liu, 2003; Monaghan, 1992). A major advantage of SPH is that their physical interpretation is relatively simple.

In the SPH model, the fluid is represented by a discrete set of N particles. The position of the ith particle is denoted by the vector r_i, i=1,…, N. We start introducing the function $A_s(r)$, that is the smoothed representation of any arbitrary function A(r) (the function A(r) is any physical quantity of the hydrodynamical model and $A_s(r)$ is the smoothed version of this quantity). The SPH scheme is based on the idea of a smoothed representation $A_s(r)$ of the continuous function A(r) that can be obtained from the convolution integral

$$A_S(\mathbf{r}) = \int A(\mathbf{r}')W(\mathbf{r} - \mathbf{r}', h)d\mathbf{r}'. \tag{1}$$

Here h is the smoothing length, and the smoothing function W satisfies the normalization condition

$$\int W(\mathbf{r} - \mathbf{r}', h)d\mathbf{r}' = 1. \tag{2}$$

The integration is performed over the whole space. In the limit of h tending to zero, the smoothing function W becomes a Dirac delta function, and the smoothed representation $A_s(r)$ tends to A(r).

In the SPH scheme, the properties associated with particle i, are calculated by approximating the integral in eq. (1) by the sum

$$A_i = \sum_j \Delta V_j A_j W(\mathbf{r}_i - \mathbf{r}_j, h)$$
$$= \sum_j m_j \frac{A_j}{\rho_j} W(\mathbf{r}_i - \mathbf{r}_j, h). \tag{3}$$

Here ΔV_j is the fluid volume associated with particle j, and m_j and ρ_j are the mass and density of the jth particle, respectively. In equation (3), A_j is the value of a physical field A(r) on the particle j, and the sum is performed over all particles. Furthermore, the gradient of A is calculated using the expression

$$\nabla A_i = \sum_j m_j \frac{A_j}{\rho_j} \nabla_i W(\mathbf{r}_i - \mathbf{r}_j, h). \tag{4}$$

In the equation (3), ρ_i/m_i can be replaced by the particle number density $n_i = \rho_i/m_i$, so that

$$A_i = \sum_j \frac{A_j}{n_j} W(\mathbf{r}_i - \mathbf{r}_j, h). \tag{5}$$

The particle number density can be calculated using the expression

$$n_i = \sum_j W(\mathbf{r}_i - \mathbf{r}_j, h). \tag{6}$$

The mass density is given by

$$\rho_i = \sum_j m_j W(\mathbf{r}_i - \mathbf{r}_j, h). \tag{7}$$

Similarly, the gradient can be calculated using the expression

$$\nabla A_i = \sum_j \frac{A_j}{n_j} \nabla_i W(\mathbf{r}_i - \mathbf{r}_j, h). \tag{8}$$

The SPH discretization reduces the Navier-Stokes equation to a system of ordinary differential equations having the form of Newton's second law of motion for each particle. This simplicity allows taking into account a variety of chemical effects with relatively little effort in the development of computational codes. Also, since the number of particles remains constant in the simulation and the interactions are symmetrical, the mass, momentum and energy are conserved exactly, and the systems like dynamic boundaries and interfaces can be modeled without too much difficulty. Hoover (1998), and Colagrossi & Landrini (2003), used the SPH method to model immiscible flows and found that the standard formulation of SPH proposed by Gingold & Monaghan (1977) creates an artificial surface tension on the border between the two fluids. Colagrossi & Landrini (2003) put forward an SPH formulation for the simulation of interfacial flows, that is, flow fields of different fluids separated by interfaces. The scheme proposed for the simulation of interfacial flows starts considering that the fluid field is represented by a collection of N particles interacting with each other according to evolution equations of the general form

$$\frac{d\rho_i}{dt} = -\rho_i \sum_j M_{ij},$$

$$\frac{d\mathbf{u}_i}{dt} = -\frac{1}{\rho_i} \sum_j \mathrm{F}_{ij} + f_i, \tag{9}$$

$$\frac{d\mathbf{x}_i}{dt} = \mathbf{u}_i.$$

The terms M_{ij} and F_{ij} arise from the mass and momentum conservation equations. In the equations (9) appear the density ρ_i, the velocity u_i of the particles, and the force f_i can be any body force. When there are fluid regions with a sharp density gradient (interfaces), the SPH standard formulations must be modified in order to be applied to treat such systems. This difficulty can be circumvented using the following discrete approximations

$$div(\mathbf{u}_i) = \sum_j (\mathbf{u}_j - \mathbf{u}_i) \cdot \nabla W_{ji} \frac{m_j}{\rho_j},$$

$$\nabla A_i = \sum_j (A_j - A_i) \nabla W_{ji} \frac{m_j}{\rho_j}. \tag{10}$$

Here W is the Kernel or Smoothing Function and A can be any scalar field or continuous function. The small difference between the equation (10) and the standard equation that uses

m_j/ρ_i instead m_j/ρ_j is important for the treatment of the case of small density ratios. On the other hand, it can be shown that the pressure gradient can be written as

$$\nabla p_i = \sum_j (p_j + p_i) \nabla W_{ji} dV_j.$$ (11)

The equation (11) is variationally consistent with eq. (10). In this scheme the terms M_{ij} and F_{ij} appearing in eq. (9) are given by the expressions

$$M_{ij} = (u_j - u_i) \cdot \nabla W_{ji} \frac{m_j}{\rho_j},$$

$$F_{ij} = (p_j + p_i) \nabla W_{ji} \frac{m_j}{\rho_j}.$$ (12)
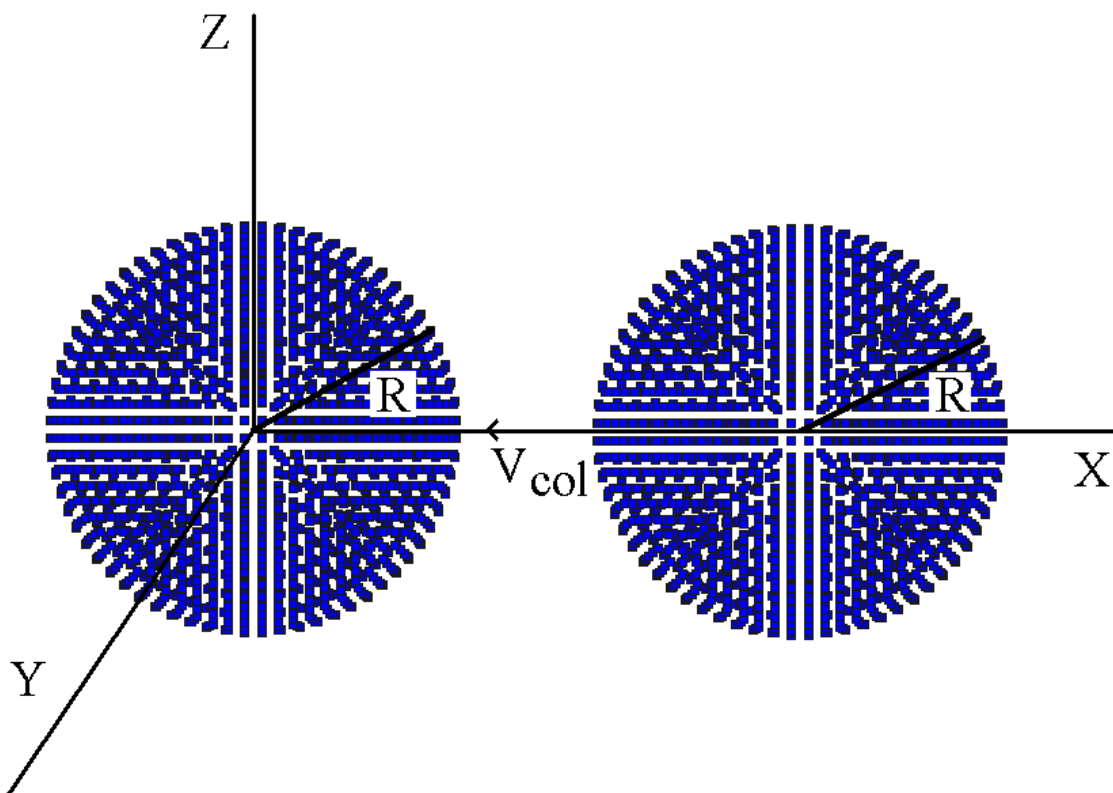
Fig. 1. Definition of the problem: head-on coalescence collision in three dimensions between two drops of equal size approaching with a velocity of collision V_{col} and radius R in empty space. Each drop is composed by 4700 SPH particles.

A density re-initialization is needed when each particle has a fixed mass, and when the number of particles is constant the mass conservation is satisfied. Yet if one uses eq. (9) for the density, the consistency between mass, density and occupied area is not satisfied. To solve this problem, the density is periodically re-initialized applying the expression

$$\rho_i = \sum_j m_j W_{ij}.$$ (13)

In this formulation special attention must be paid to the kernel. In fact depending on which kernel is used, eq. (13) could introduce additional errors. For this reason a first-order interpolation scheme is suitable to re-initialize the density field by using the equation

$$\left\langle \rho_i \right\rangle = \sum_j \rho_j W_j^{MLS}(x_i) dV_j = \sum_j m_j W_j^{MLS}(x_i), \tag{14}$$

Where W_j^{MLS} is the moving-least-square kernel.

The XSPH (Extended Smoothed Particle Hydrodynamics, which is a variant of the SPH method for the modeling of free surface flows (Monaghan, 1994)) velocity correction Δu_i is introduced to prevent particles inter-penetration (Colagrossi & Landrini, 2003), which takes into account the velocity of the neighbor particles using a mean value of the velocity, according to the equations

$$\left\langle \mathbf{u}_i \right\rangle = u_i + \Delta u_i, \quad \Delta u_i = \frac{\varepsilon'}{2} \sum_j \frac{m_j}{\overline{\rho}_{ij}} (u_j - u_i) W_{ji}, \tag{15}$$

where $\overline{\rho}_{ij}$ is the mean value of density between the ith and jth particle, and ε' is the relative change of an arbitrary quantity between simulations (Colagrossi & Landrini, 2003).

The velocity and acceleration fields are (Liu & Liu, 2003)

$$\frac{d\mathbf{r}_i}{dt} = \mathbf{v}_i,$$

$$\frac{d\mathbf{v}_i^\alpha}{dt} = \sum_{j=1}^N m_j \left(\frac{\sigma_i^{\alpha\beta}}{\rho_i^2} + \frac{\sigma_j^{\alpha\beta}}{\rho_j^2} \right) \cdot \nabla W_{ij}^h, \tag{16}$$

where σ is the total stress tensor.

The internal energy evolution is given by the expression (Liu & Liu, 2003) :

$$\frac{dE_i}{dt} = \frac{1}{2} \sum_{j=1}^N m_j \left(\frac{p_i}{\rho_i^2} + \frac{p_j}{\rho_j^2} \right) \left(\mathbf{v}_i^\beta - \mathbf{v}_j^\beta \right) \frac{\partial W_{ij}}{\partial x_i^\beta} + \frac{\mu_i}{2\rho_i} \varepsilon_i^{\alpha\beta} \varepsilon_i^{\alpha\beta}, \tag{17}$$

In the above equation p is the pressure, μ is the dynamic viscosity and ε is the shear strain rate.

In the present work, our calculations are performed in three dimensions and we use the cubic B-spline kernel (Monaghan, 1985). We consider water drops, and the equation of state that we use in the hydrodynamical code was a general Mie-Gruneisen form of equation of state with different analytic forms for states of compression $(\rho/\rho_0 - 1) > 0$ and tension $(\rho/\rho_0 - 1) < 0$ (Liu & Liu, 2003). This equation has several parameters, namely the density ρ, the reference density ρ_0, and the constants A_1, A_2, A_3, C_1 and C_2. The pressure P is

$$P = A_1 \left(\frac{\rho}{\rho_0} - 1 \right) + A_2 \left(\frac{\rho}{\rho_0} - 1 \right)^2 + A_3 \left(\frac{\rho}{\rho_0} - 1 \right)^3 \quad if \quad \left(\frac{\rho}{\rho_0} - 1 \right) > 0 \tag{18}$$

and

$$P = C_1\left(\frac{\rho}{\rho_0} - 1\right) + C_2\left(\frac{\rho}{\rho_0} - 1\right) \quad if \quad \left(\frac{\rho}{\rho_0} - 1\right) < 0. \tag{19}$$

In all our calculations we use the following values for the constants: A_1=2.20x10^6 kPa, A_2=9.54x10^6 kPa, A_3=1.46x10^7 kPa, C_1=2.20x10^6 kPa, C_2=0.00 kPa, and ρ_0=1000.0 Kg/m^3.

3. Coalescence, fragmentation and flocculation of liquid drops in three dimensions

In order to model the collision of liquid drops several calculations were carried out. We have varied the velocity of collision for modeling the permanent coalescence of droplets in the three dimensional space (3D) in a vacuum environment using the SPH method. In order to proceed we have defined drops with diameter of 30µm and 4700 SPH particles for each drop with a collision velocity of 1.0 mm/ms.

In figure 2 is illustrated a sequence of times showing the evolution of the collision between two drops (permanent coalescence) with V_{col} = 1.0 mm/ms and We= 4.5. The evolution of time is shown in milliseconds. It can be seen in this figure that at t=0.0009 ms a flat circular section appears (Ivanov & Kralchevsky, 1997), which increases its diameter as dynamics progresses. The appearance of this flat circular section has been reported for the case of collision of drops in emulsion media (Ivanov & Kralchevsky, 1997), yet in this reference the hydrodynamic modeling of the collision of liquid drops is not considered. In the dynamics we observe that at t = 0.0053 ms a bridge structure between the two drops appears in the region of contact (this bridge is the structure that joins the drops through their flat circular interfaces placed in the center of the droplets coalescence), which disappears at a later time due to the penetration of particles of one drop into the other. After that, a process of coalescence occurs (see figure 2 at t=0.0069 ms) and a bigger drop is formed (see figure 2 at t=0.0077ms).

Figure 3 shows the velocity vector field inside the droplets and in the region of contact between them at t=0.004ms. Notice that inside the drops, the fluid tends to a velocity value lower than the initial velocity of 1.00 mm/ms, while in the area of contact between the drops we observe an increase in the fluid velocity to a value of 1.436 mm/ms. Once the coalescence process occurs, the velocity of the fluid inside the drops tends to zero, i.e. the largest drop size that is formed after some time tends to equilibrium. This can be seen in figure 4 where it is illustrated the time evolution of the kinetic and internal energy of the bigger drop. When two drops collide the possible results of the collision (coalescence, flocculation or fragmentation of drops) depends only on the kinetic energy and the Weber number (We) (Foote, 1974), which is given by

$$We = \frac{\rho V_r^2 d}{\sigma}. \tag{20}$$

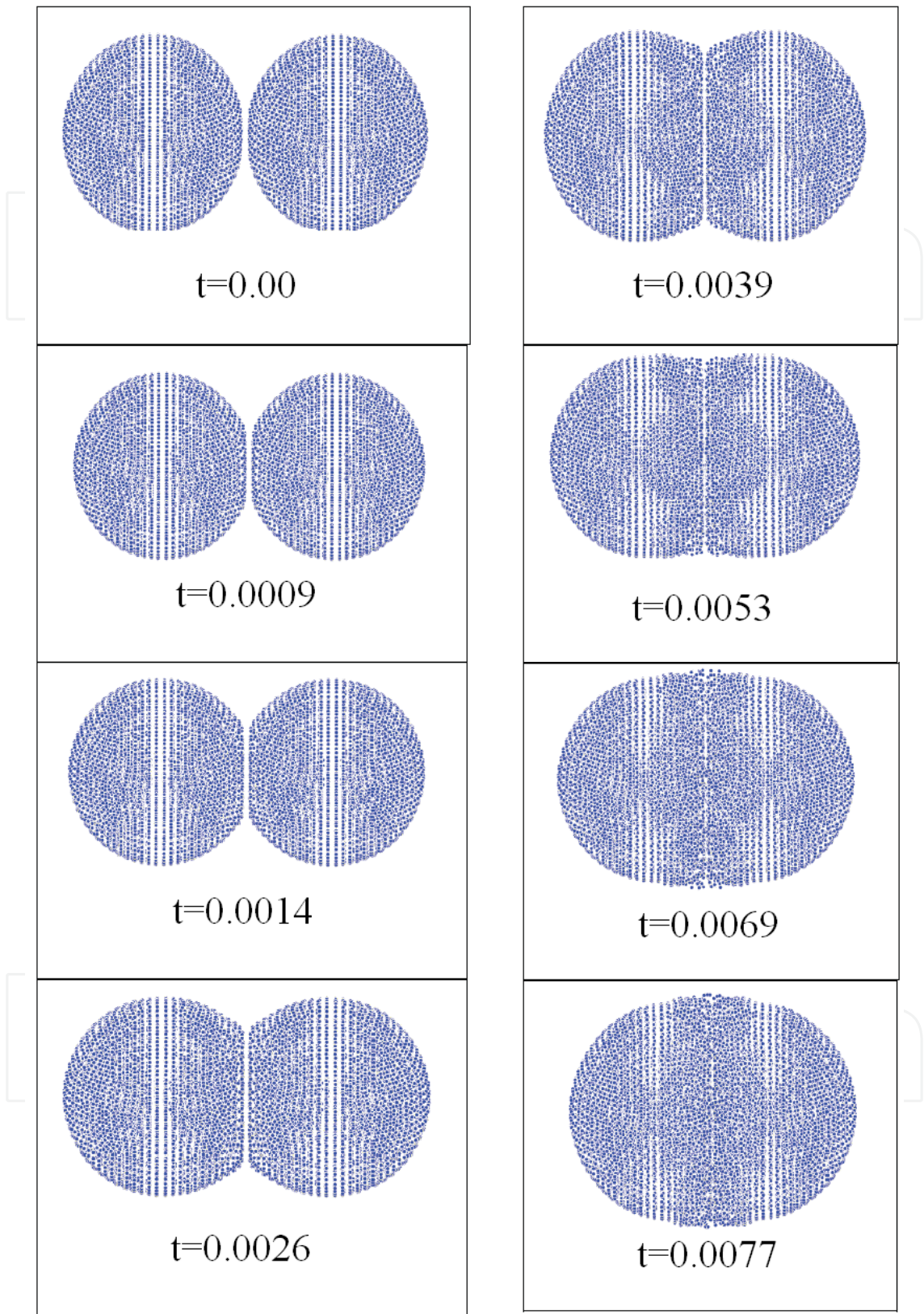Here Vr is the difference between the velocities of the drops, d the diameter of the drop, and σ the surface tension.

Fig. 2. Sequence of times showing the evolution of the collision between two drops (permanent coalescence) with V_{col} = 1.0 mm/ms and We = 4.5. The time scale is given in milliseconds.

From the values of density, relative velocity, droplet diameter and surface tension we obtain the Weber number. The Surface tension σ is determined using the Laplace equation

$$\left[p(r=0)-p(r\rightarrow\infty)\right]=\frac{\sigma}{R}. \tag{21}$$

The first term p (r = 0) on the left side of the equation (21) is determined at the drop center and the second term p (r → ∞) is taken as the vanishing pressure far away from the drop. The calculations were made in a vacuum environment and only head-on collisions were considered. The value of the pressure at the drop center is 1.78kPa and the Weber number for the coalescence collision is We=4.5. Values of the Weber number in the range 1≤We≤19 have been chosen, which corresponds to the range reported by Ashgriz & Poo (1990) for experimental head-on collisions and coalescence of water drops.
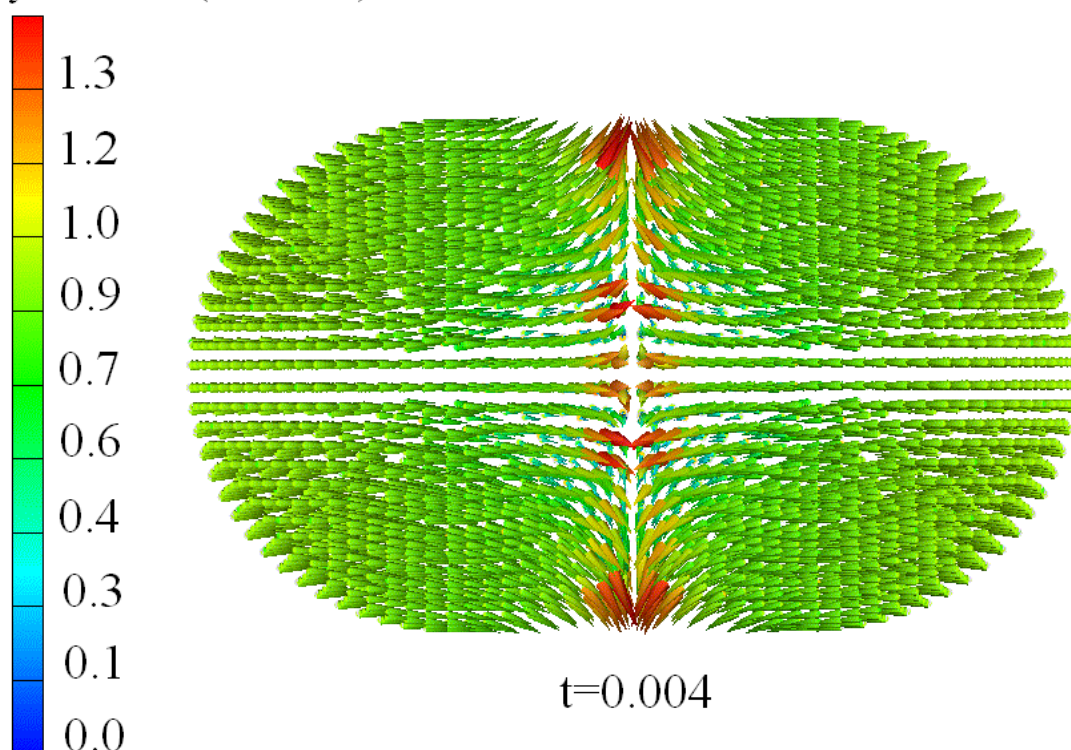
Fig. 3. Velocity vector field for the collision between two drops at t=0.004 ms (permanent coalescence process) with V_{col} = 1.0 mm/ms and We = 4.5. The time scale is given in milliseconds.

The coalescence processes occurring in droplets collision at low Weber numbers illustrated in the figures 1, 2 and 3 are governed by the competition between stretching and drop drainage. This drainage occurs when the liquid flows from the high-pressure drop region toward the point of contact to form a liquid bridge.

For larger values of We, the initially merged droplets would subsequently split apart, with the simultaneous production of smaller satellite droplets. It can be observed in our simulations (see figure 2) that the circular flat section disappears. Also, due to the effect of the surface tension a structure having the form of bridge is observed at t=0.0053ms and the

permanent coalescence occurs. The outcomes reported by Qian & Law (1997) are in good agreement with our results. In our SPH calculation, the relative velocity is not enough to produce fragmentation of the bigger drop and subsequently to produce small satellite droplets. In this calculation, the coalescence is permanent and the bigger drop that is formed reaches the equilibrium (see figure 4). On the other hand, the experiments of Qian & Law (1997) do not have a sufficient resolution to show in detail the deformation of the drops just before the formation of the bridge. However, the appearance of the flat circular section shown in figure 2 is in good agreement with the experimental and theoretical outcomes reported in the literature (Bibette et al., 1992; Ivanov & Dimitrov, 1988; Ivanov & Kralchevsky, 1997; Kabalnov & Wennerström, 1996; Sharma & Ruckenstein, 1987).
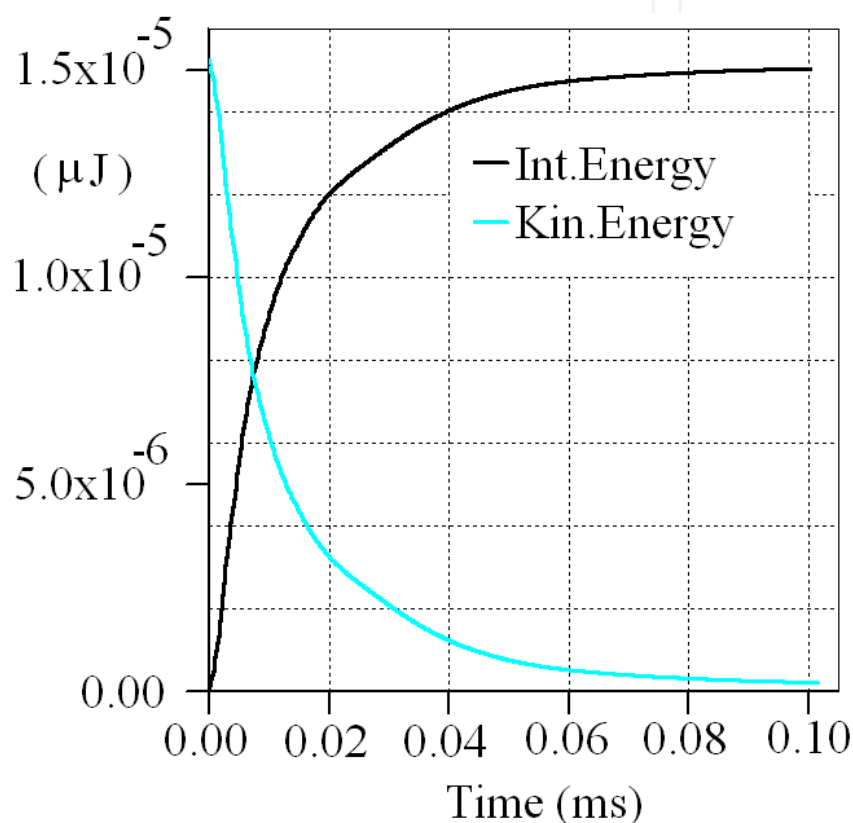

Fig. 4. Evolution of the Kinetic and Internal energy for the collision between two equal-sized drops with V_{col} = 1.0 mm/ms and We = 4.5.

On the other hand, it is observed that if we choose a Weber number for the collision greater than the range of values producing permanent coalescence, the phenomenon of fragmentation arises, i.e. the regime 2 reported by Qian & Law (1997) occurs giving rise to coalescence followed by separation into small satellite drops. The following calculations were performed for droplets with 30μm of diameter, 4700 SPH particles for each drop, and a collision velocity of 10.0 mm/ms (We=450) which is a characteristic velocity for the elements of a liquid spray (Choo & Kang, 2003). In the first stage of the calculation at t=2.0x10⁻⁴ms the collision of the two droplets is shown in figure 5. It can be seen the formation of a flat circular section between the drops (Ivanov & Kralchevsky, 1997). This circular section vanishes completely at t = 5.6 x10⁻⁴ms. At this time a portion of fluid appears to form a wave front propagating in the plane x = 0.

This wave front begins to form little satellite drops and increases its amplitude until t=1.8x10^{-3}ms. There is no substantial growth of these satellite drops and the structure tends to a flatten form as the dynamic runs. Figure 6 shows the velocity vector field (seen from the plane y = 0) after the fragmentation of the drops has taken place. As shown in figure 6, the fluid velocity at the center of the structure is 8.7 mm/ms, which is less than the initial rate of collision, while the fluid that is spread to the edges is accelerated reaching a speed of 15.0 mm/ms. A longer stretched ligament is produced and the amount of satellite droplets increases with the evolution of dynamics. Figure 5 illustrates that a portion of the fluid begins to separate, stretching away from the bigger drop, and a non-uniform pressure field is created inside the ligament. This is related to the value in the velocity vector field differences, and due to this pressure differential a flow parallel to the plane x=0 is produced. The fragmentation phenomena and the subsequent formation of satellites drops may be analyzed following the conjectures made by Qian & Law (1997).

Once the ligament begins to form (see figure 5), a flow is generated directed in the opposite direction to the vector field shown in figure 6. This motion transform this portion of the ligament in a bulbous due to the accumulation of mass in this volume, and this change in geometry implies the appearance of a local minimum in the pressure field which is located between the bulbous and its neighboring region.

As a result of this pressure difference a local flow is generated through the point of minimum pressure that opposes to the flow that is coming from the bulbous. This fluid motion causes a local reduction of mass and therefore the ligament between the bulbous and the neighboring region starts to decrease its radius (at the point of minimal pressure). Because of this local decrease of the ligament radius the pressure rises, which creates a flow with the same direction of the flow that comes from the end of the bulbous and other flow in the opposite direction from the point of local reduction of mass. Given these opposing flows emerging from this point, the radius of the ligament decreases even more. Then the system tends to relax this unstable situation reducing the radius of this region to zero, giving rise to a division of the fluid and so producing a satellite drop (see figure 5). Subsequently, this process is repeated in the other regions of the ligament, producing more satellites drops. These shattering collisions occur only at high velocities making the surface tension forces of secondary importance (the phenomenon is inertial dominated).

When the Weber number for the collision is decreased below the range corresponding to the permanent coalescence regime, then flocculation occurs. These calculations were performed for droplets with 30μm of diameter, 4700 SPH particles for each drop, and a collision velocity of 0.2mm/ms (We=0.18). At the beginning of the calculation one observes at t=0.29ms (see figure 7) that a flat circular section appears between the two droplets (Ivanov & Kralchevsky, 1997), which has already increased in diameter at t=1.0ms. Then, there is a stretching of the surface of the drop as can be seen at t=1.77ms. This stretch is deforming the drops until t=3.76 ms, and after that the drop shape remains constant. The chosen collision velocity cannot produce coalescence between the droplets. In fact no penetration was observed through the plane x=0. In this case, only the drops stay together, interacting through their surfaces, giving rise to flocs (Ivanov & Kralchevsky, 1997).

It has been reported that these flocs are formed in emulsions when the interfacial film between drops is very stable or the drops approach each other with a very small kinetic energy (Ivanov & Dimitrov, 1988; and Ivanov & Kralchevsky, 1997). In this case, the wave front that appears in the plane x=0 of figure 5 was not observed. Figure 8 shows the velocity vector field at t = 1.78ms. It can be seen in this figure that the value of the fluid velocity
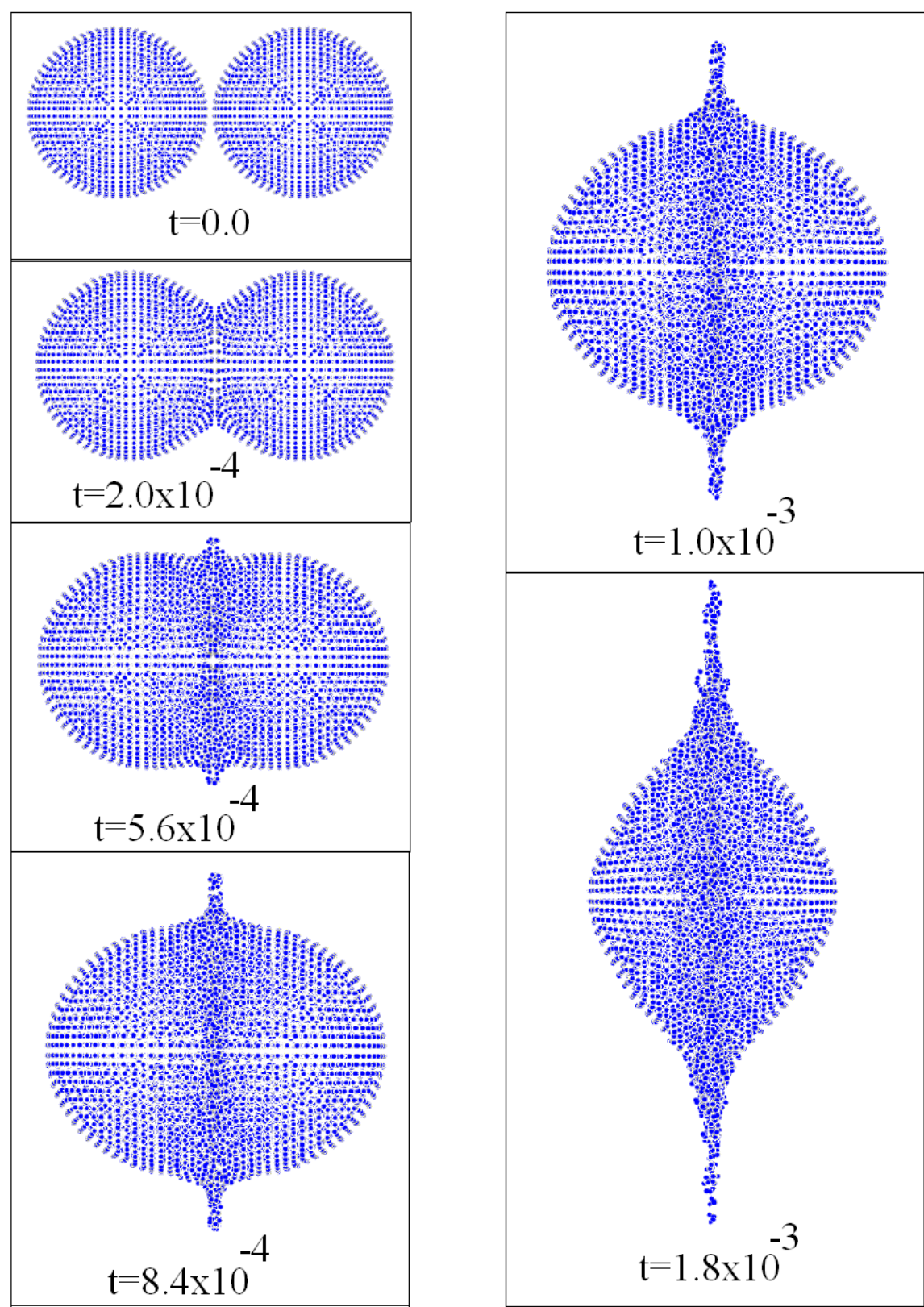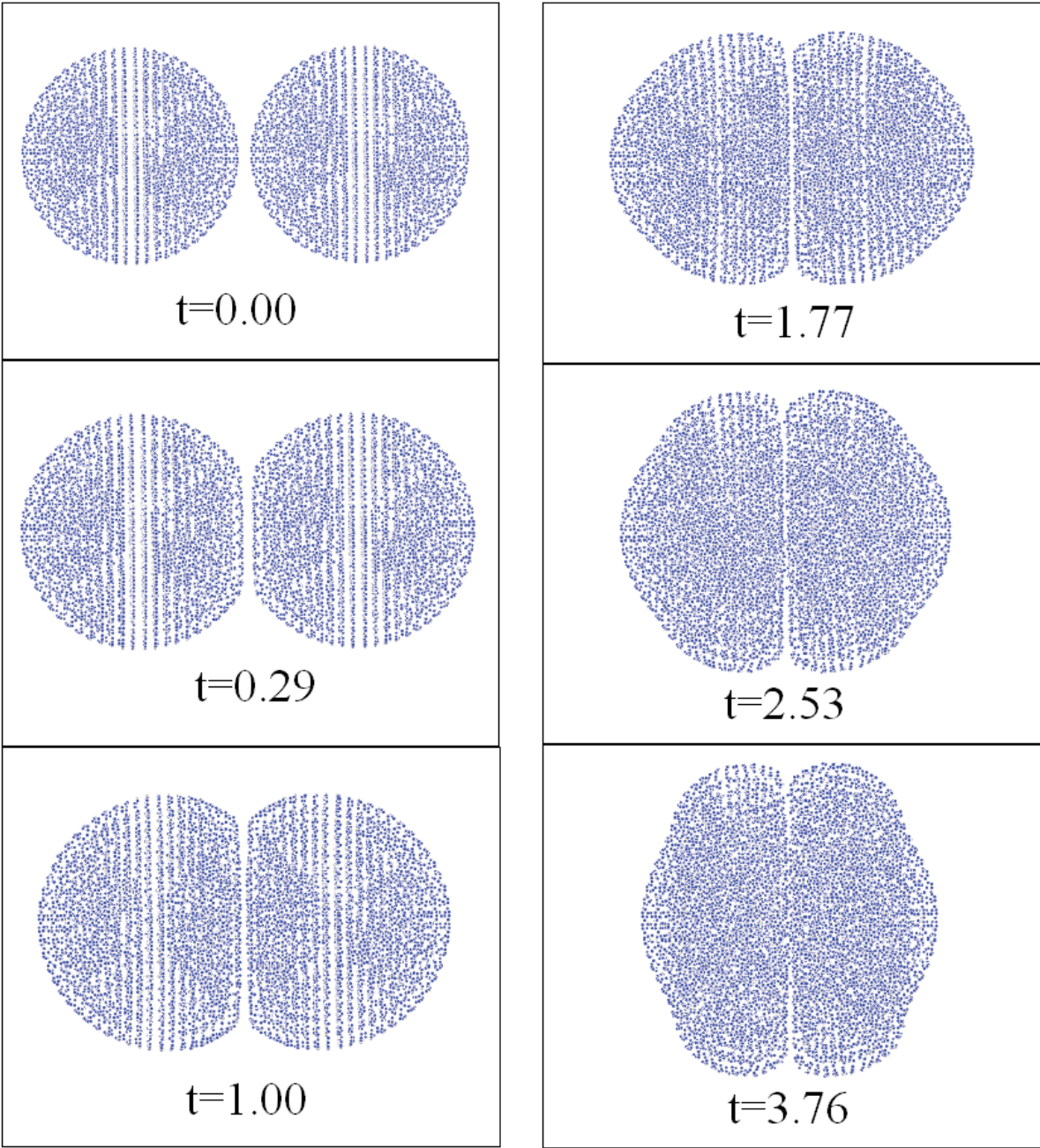
Fig. 5. Sequence of times showing the evolution of the collision between two drops with V_{col} = 10.0 mm/ms and We = 450. This figure illustrates the formation of small satellite droplets. The time scale is given in milliseconds.

decreases from the border to the center of the drop. In this case, the velocity has decreased below its initial value, which is 0.2mm/ms in all zones of the fluid. As is shown in figure 9, after an elapsed time of 3.76ms, the fluid velocities decrease even more, reaching a value of 2.24×10^{-2} mm/ms in the zone of interaction between the two drops and 4.48×10^{-2} mm/ms near the border.
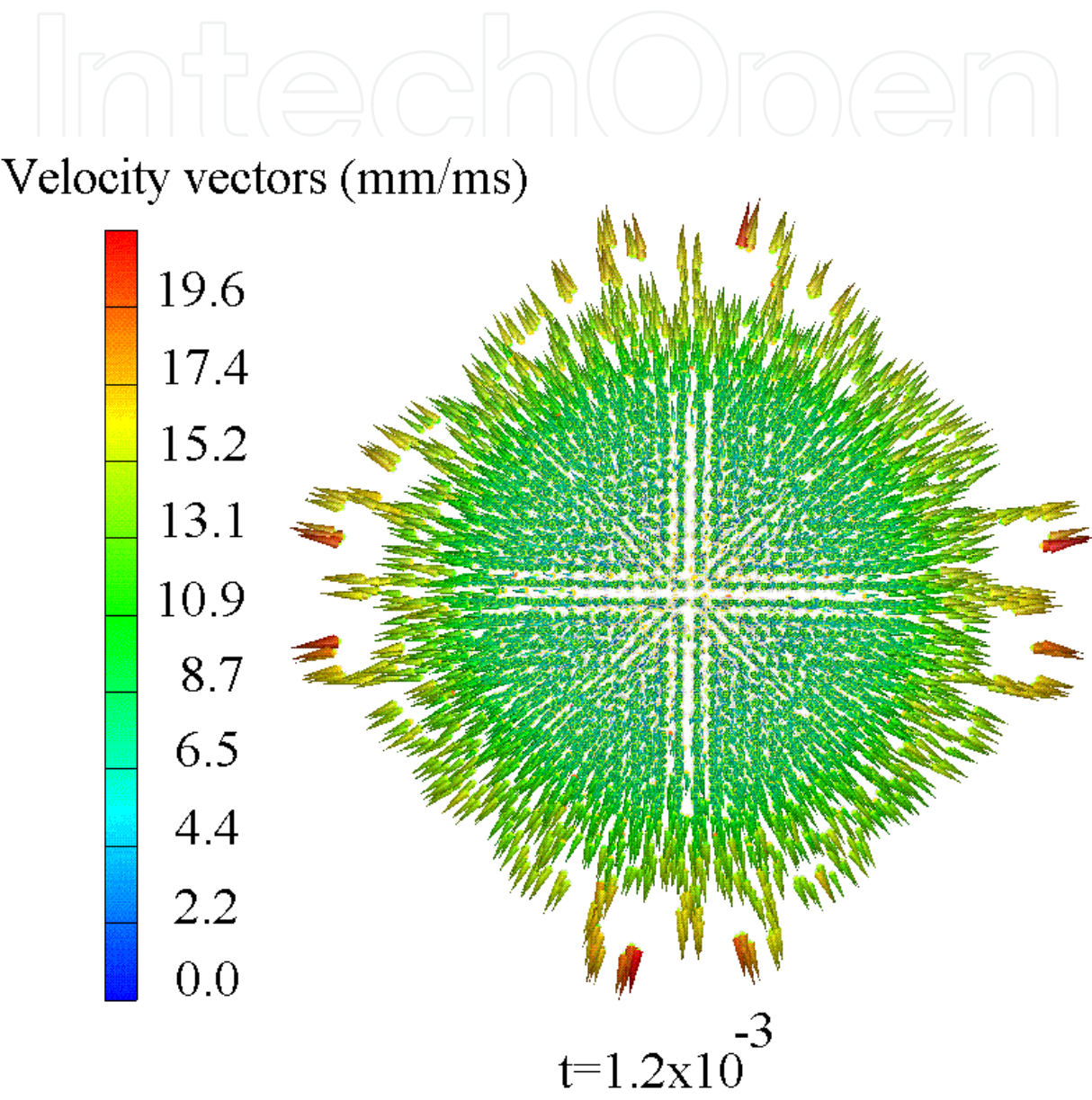
Fig. 6. Velocity vector field showing the fragmentation of two colliding drops at $t=1.2\times10^{-3}$ms (see from the plane z-x) with V_{col}=10.0 mm/ms and We = 450. The time scale is given in milliseconds.

Fig. 7. Sequence of times showing the evolution of the collision between two drops (flocculation) with V_{col} = 0.2 mm/ms and We = 0.18. The time scale is given in milliseconds.
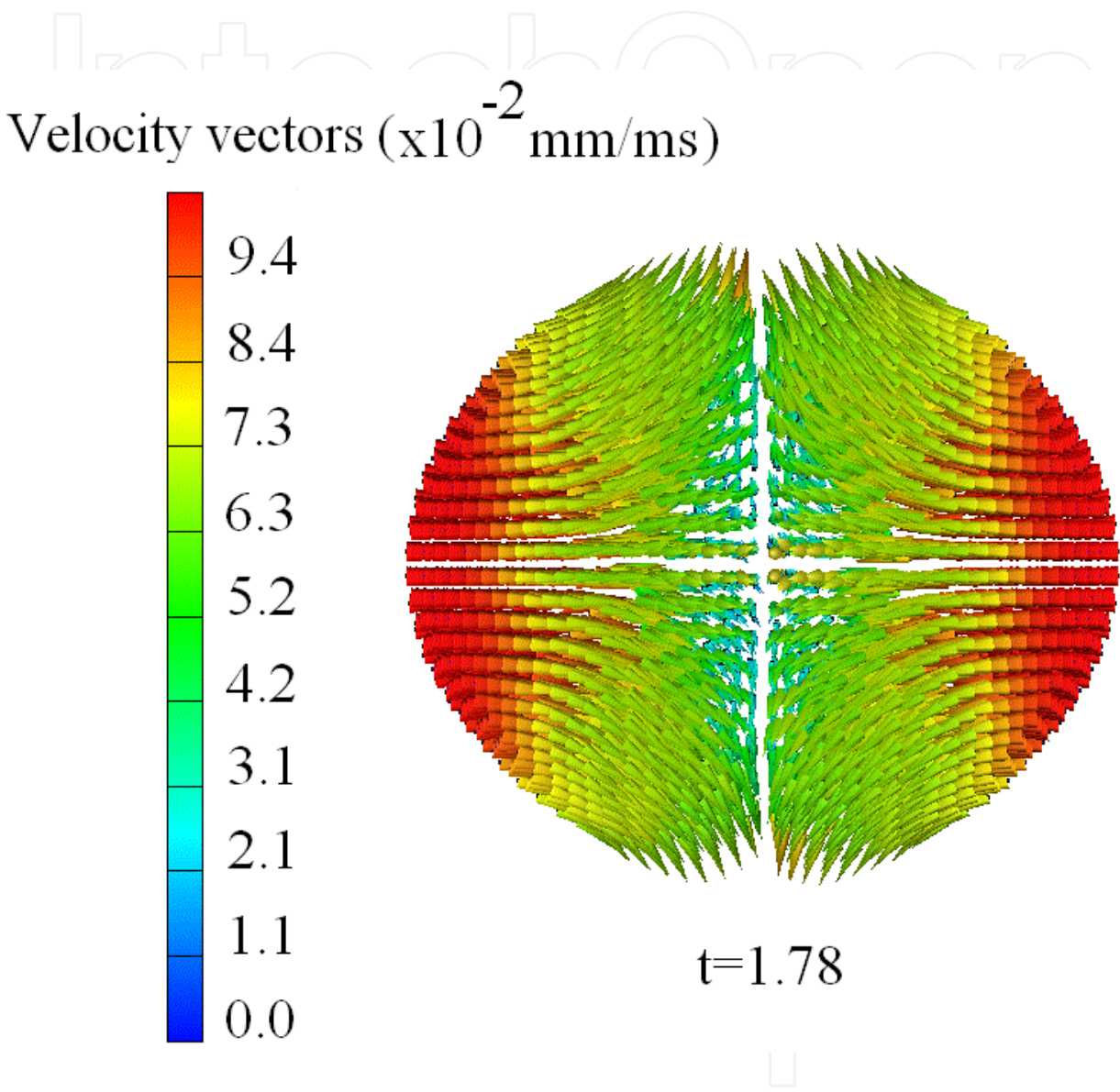
Fig. 8. Velocity vector field showing the flocculation of two liquid drops at t=1.78 ms with V_{col} = 0.2mm/ms and We = 0.18. The time scale is given in milliseconds.

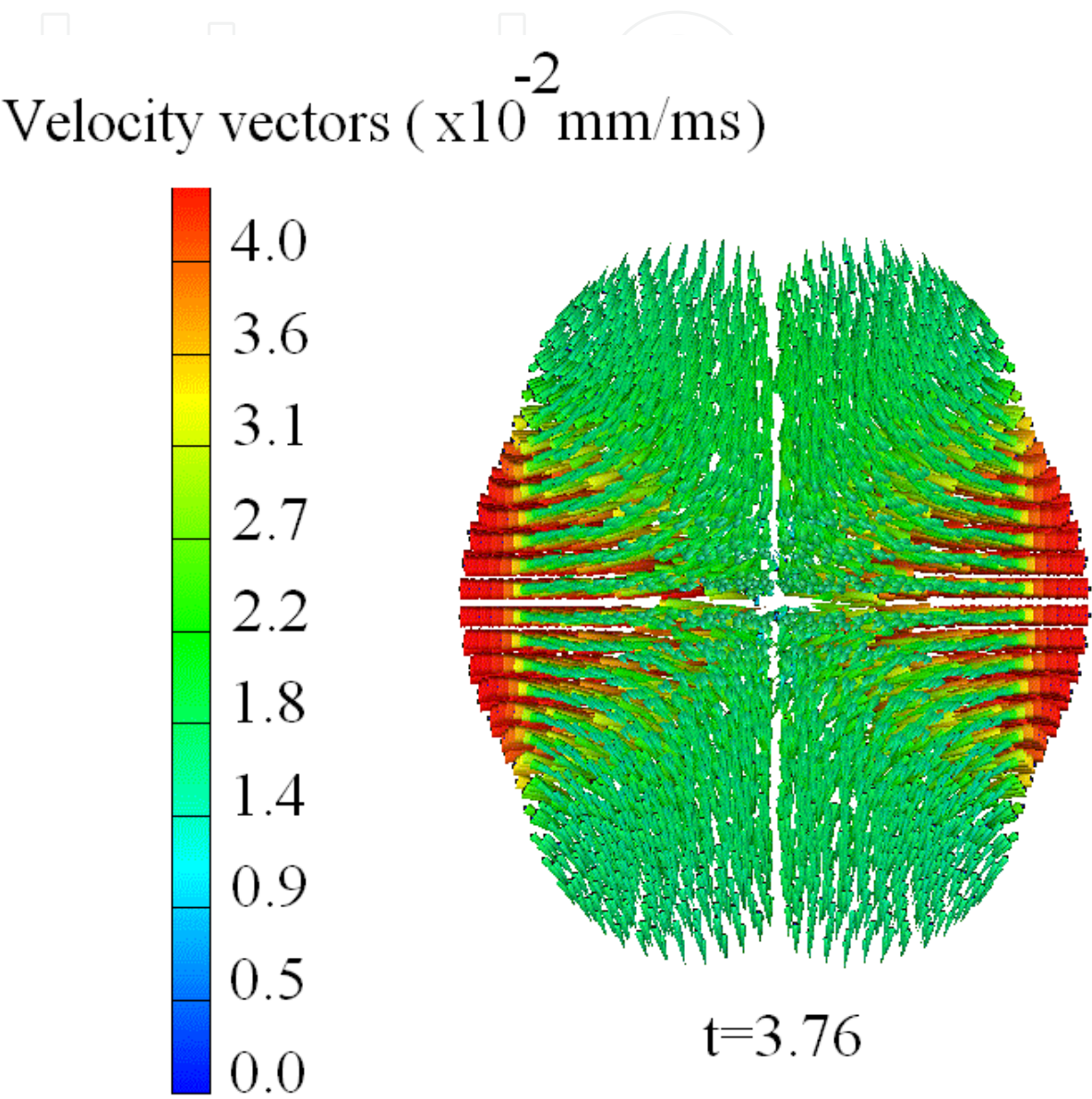Fig. 9. Velocity vector field showing the flocculation of two liquid drops at t=3.76 ms with V_{col} = 0.2mm/ms and We = 0.18. The time scale is given in milliseconds.

4. Conclusions

An adequate methodology using the SPH method in three-dimensional space was presented for the calculation of hydrodynamic collisions of liquid drops in a vacuum environment. Several features of binary collisions in three dimensions have been observed in our calculations. As a result of the collision between droplets the formation of a circular flat film was obtained for a range of values of the Weber number. We have found three possible outcomes for the collision: permanent coalescence, fragmentation and flocculation of drops. We have ascribed a range of Weber number values for the three possible outcomes of the collisions.

Inside the drops, the fluid tends to a velocity value lower than the initial velocity of collision, while in the area of contact between the drops, we observed an increase in the fluid velocity. When the Weber number of the drops is larger than the range of values corresponding to coalescence, a fragmentation phenomenon is observed. Otherwise, when the Weber number is below this range, we obtained drop flocculation. In the case of drop fragmentation, we have observed the formation of satellite droplets emerging from the contact zone between the two drops. The mechanism of formation of these satellite droplets has been discussed.

We can see in the velocity vector field that after the fragmentation of the drops has taken place, the fluid velocity at the center of the structure is less than the initial rate of collision, while the fluid that is spread to the edges is accelerated producing a long stretched ligament and several satellite droplets. In the SPH dynamics that the drops follow when flocculation occurs, we have obtained that the system tends to a state of equilibrium in which the kinetic energy remains constant and the drops interact mainly through their deformed surfaces. On the velocity vector fields can be seen that in this case the value of the fluid velocity decreases from the border to the center of the drops. In all zones of the fluid the velocity has decreased below its initial value. After an elapsed time the fluid velocities decrease even more in the zone of interaction between the two drops near the border.

5. References

Ashgriz, N. & Givi, P. (1987). Binary collision dynamics of fuel droplets. *Int. J. Heat Fluid Flow,* 8, 1987, pp. 205-208;

Ashgriz, N. & Givi, P. (1989). Coalescence efficiencies of fuel droplets in binary collisions. *Int. Commun. Heat Mass Transfer,* 16, 1989, pp. 11-17;

Ashgriz, N. & Poo, J.Y. (1990). Coalescence and separation of binary collisions of liquid drops. *J. Fluid Mech.,* 221, 1990, pp. 183-204;

Azizi, F. & Al Taweel, A.M. (2010). Algorithm for the accurate numerical solution of PBE for drop breakup and coalescence under high shear rates. *Chem. Eng. Sci.,* 65, 2010, pp. 6112-6127;

Benz, W. & Asphaug. (1994). Impact simulations with fracture: I. Method and tests. *Icarus,* 1233, 1994, pp. 98-116.

Benz, W. & Asphaug. (1995). Simulations of brittle solids using smoothed particle hydrodynamics. *Comput. Phys. Commun.,* 87, 1995, pp. 253-265;

Bibette, J., Morse, D.C., Witten, T.A. & Weitz, D.A. (1992). Stability criteria for emulsions. *Phys. Rev. Lett.,* 69, 1992, pp. 2439-2443;

Bozzano, G. & Dente, M. (2010). Mechanism of drop coalescence at the interface of two immiscible liquids. 20th European Symposium on Computer Aided Process Engineering – ESCAPE20, 28, 2010, pp. 55-60;

Bradley, S.G. & Stow, C.D. (1978). Collision between liquid drops. *Philos. Trans. R. Soc. London Ser. A,* 287, 1978, pp. 635-642;

Brenn, G. & Frohn, A. (1989). Collision and merging of two equal droplets of propanol. *Exp. Fluids*, 7, 1989, pp. 441-446;

Brenn, G. & Kolobaric, V. (2006). Satellite droplet formation by unstable binary drop collisions. *Phys. Fluids*, 18, 2006, pp. 1-18;

Chen, J.D. (1985). A model of coalescence between two equal-sized spherical drops or bubbles. *J. Colloid Interface Sci.*, 107, 1985, pp. 209-220;

Choo, Y.J. & Kang, B.S. (2003). A study on the velocity characteristics of the liquid elements produced by two impinging jets. *Exp. in Fluids*, 34, 2003, pp. 655-661;

Colagrossi, A. & Landrini, M. (2003). Numerical simulation of interfacial flows by smoothed particle hydrodynamics. *J. Comput. Phys.*, 191, 2003, pp. 448-475;

Cristini, V., Bawzdziewicz, J. & Loewenberg, M. (2001). An Adaptive Mesh Algorithm for Evolving Surfaces: Simulations of Drop Breakup and Coalescence. *J. Comput. Phys.*, 168, 2001, pp. 445-463;

Cui, J., He, G.W. & Qi, D.W. (2006). A constrained particle dynamics for continuum-particle hybrid method in micro- and nano fluidics. Acta Mechanica Sinica, 22, 2006, pp. 503-508;

Decent, S.P., Sharpe, G., Shaw, A.J. & Suckling, P.M. (2006). The formation of a liquid bridge during the coalescence of drops. Int. J. *Multi-phase Flow*, 32, 2006, pp. 717-738;

Desbrun, M. & Gascuel, M.P. (1996). Smoothed Particles: a new paradigm for animating highly deformable bodies. *Proceedings of Eurographics Workshop on animation and simulation*, 1996.

Duchemin, L., Eggers, J. & Josserand, C. (2003). Inviscid coalescence of drops. *J. Fluid Mech.*, 487, 2003, pp. 167-180;

Eggers, J., Lister, J.R. & Stone, H.A. (1999). Coalescence of liquid drops. *J. Fluid Mech.*, 401, 1999, pp. 293-310;

Foote, G.B. (1974). The water drop rebound problem: Dynamics of collision. *J. Atmos. Sci.*, 32, 1974, pp. 390-401;

Gingold, R.A. & Monaghan, J.J. (1977). Smoothed particle hydrodynamics: theory and application to non-spherical stars. *Roy. Astronom. Soc.*, 181, 1977, pp. 375-389;

Gokhale, S.J., Dasgupta, S., Plawsky, J.L. & Wayner, P.C. (2004). Reflectivity-based evaluation of the coalescence of two condensing drops and shape evolution of the coalesced drop. *Phys. Rev. E.*, 70, 2004, pp. 1-12;

Gotaas, C., Havelka, P., Jakobsen, H., Svendsen, H., Hase, M., Roth, N. & Weigand, B. (2007, a). Effect of viscosity on droplet-droplet collision outcome: Experimental study and numerical comparison. *Phys. Fluids*, 19, 2007, pp. 1-17;

Gotaas, C., Havelka, P., Jakobsen, H. & Svendsen, H. (2007, b). Evaluation of the impact parameter in droplet-droplet collision experiments by the aliasing method. *Phys. Fluids*, 19, 2007, pp. 1-14;

Hoover, W.G. (1998). Isomorphism linking smooth particles and embedded atoms. *Physica A*, 260, 1998, pp. 244-255;

Ivanov, I.B. & Dimitrov, D.S. (1988). Thin Liquid Films Fundamentals and Applications. Dekker, 1988.

Ivanov, I.B. & Kralchevsky, P.A. (1997). Stability of emulsions under equilibrium and dynamic conditions. *Coll. Surf. A*, 128, 1997, pp. 155-175;

Jia, X., McLaughlin, J.B. & Kontomaris, K. (2006). Lattice Boltzmann simulations of drop coalescence and chemical mixing. *Physica A*, 362, 2006, pp. 62-67;

Jiang, Y.J., Umemura, A. & Law, C.K. (1992). An experimental investigation on the collision behaviour of hydrocarbon droplets. *J. Fluid Mech.*, 234, 1992, pp. 171-190;

Kabalnov, A. & Wennerström, H. (1996). Macroemulsion stability: The oriented wedge theory revisited. *Langmuir*, 12, 1996, pp. 276-292;

Koumoutsakos, P. (2005). Multiscale flow simulation using particle. *Ann. Rev. Fluid Mech.*, 37, 2005, pp. 457-487.

Leal, L.G. (2004). Flow induced coalescence of drops in a viscous fluid. *Phys. Fluids*, 16, 2004, pp. 1833-1851;

Li, D. (1994). Coalescence between two small bubbles or drops. *J. Colloid Interface Sci.*, 163, 1994, pp. 108-119;

Li, J., Liao, D. & Yip, S. (1998). Coupling continuum to molecular-dynamics simulation: reflecting particle method and the field estimator. *Phys. Rev. E*, 57, 1998, pp. 7259-7267;

Liu, G.R. & Liu, M.B. (2003). Smoothed Particle Hydrodynamics – A Meshfree Particle Method. World Scientific, 2003;

Lucy, L.B. (1977). A numerical approach to the testing of the fission hypothesis. *Astron. J.*, 82, 1977, pp. 1013-1024;

Mashayek, F., Ashgriz, N., Minkowycz, W.J. & Shotorban, B. (2003). Coalescence collision of liquid drops. *Int. J. Heat Mass Trans.*, 46, 2003, pp. 77-89;

Menchaca-Rocha, A., Huidobro, F., Martinez-Davalos, A., Michaelian, K., Perez, A., Rodriguez, V. & Carjan, N. (1997). Coalescence and fragmentation of colliding mercury drops. *J. Fluid Mech.*, 346, 1997, pp. 291-318;

Menchaca-Rocha, A., Martinez-Davalos, A., Nuñez, R. (2001). Coalescence of liquid drops by surface tension. *Phys. Rev. E.*, 63, 2001, pp. 1-5;

Mohamed-Kassim, Z. & Longmire, E.K. (2004). Drop coalescence through a liquid/liquid interface. *Phys. Fluids*, 2004, pp. 1-47;

Monaghan, J.J. (1994). Simulating Free Surface Flows with SPH. *J. Comput. Phys.*, 110, 1994, pp. 399-406;

Monaghan, J.J. (1992). Smoothed particle hydrodynamics. *Annu. Rev. Astron. Astrophys*, 1992, pp. 543-574;

Monaghan, J.J. (1985). Extrapolating B splines for interpolation. *J. Comput. Phys.*, 60, 1985, pp. 253-262;

Narsimhan, G. (2004). Model for drop coalescence in a locally isotropic turbulent flow field. *J. Coll. Interf. Sci.*, 272, 2004, pp. 197-209;

Nie, X.B., Chen, S.Y., WN, E. & Robbins, M.O. (2004). A continuum and molecular dynamics hybrid method for micro- and nano-fluid flow. *J. Fluid Mech.*, 500, 2004, pp. 55-64.

Nobari, M.R., Jan, Y.J. & Tryggvason, G. (1996). Head-on collision of drops-A numerical investigation. Phys. Fluids, 8, 1996, pp. 29-42;

O'Connell, S.T. & Thompson, P.A. (1995). Molecular dynamics-continuum hybrid computations: a tool for studying complex fluid flows. *Phys. Rev. E, 52*, 1995, pp. 5792-5795.

Pan, Y. & Suga, K. (2005). Numerical simulation of binary liquid droplet collision. *Phys. Fluids,* 17, 2005, pp. 1-14;

Park, J.Y. & Blair, L.M. (1975). The effect of coalescence on drop size distribution in an agitated liquid–liquid dispersion. *Chem. Eng. Sci.,* 30, 1975, pp. 1057-1064;

Podgorska, W. (2007). Influence of Dispersed Phase Viscosity on Drop Coalescence in Turbulent Flow. *Chem. Eng. Res. Design,* 85, 2007, pp. 721-729;

Qian, J. & Law, C.K. (1997). Regimes of coalescence and separation in droplet collision. *J. Fluid Mech.*, 331, 1997, pp. 59-80.

Roisman, L. (2004). Dynamics of inertia dominated binary drops collisions. *Phys. Fluids,* 16, 2004, pp. 3438-3449;

Roisman, L., Berberovic, E. & Tropea, C. (2009). Inertia dominated drops collisions. I. On the universal flow in the lamella. *Phys. Fluids,* 21, 2009, pp. 1-10;

Rourke, P.J. & Bracco, F.V. (1980). Modelling of drop interactions in thick sprays and a comparison with experiments, in: Stratified Charged Auto Engineering Conference. *Institute of Mechanical Engineering Publications,* 1980, pp. 101-116;

Shah, P.S., Fan, L.T., Kao, I.C. & Erickson, L.E. (1972). Modeling of growth processes with two liquid phases: a review of drop phenomena, mixing, and growth. *Adv. Appl. Microbiol.,* 15, 1972, pp. 367-414;

Sharma, A. & Ruckenstein, E. (1987). Stability, critical thickness, and the time of rupture of thinning foam and emulsion films. *Langmuir,* 3, 1987, pp. 760-768;

Sun, Z., Xi, G. & Chen, X. (2009). Mechanism study of deformation and mass transfer for binary droplet collisions with particle method. *Phys. Fluids,* 21, 2009, pp. 1-13;

Tartakovsky, A.M. & Meakin, P.A. (2005). Smoothed particle hydrodynamics model for miscible flow in three-dimensional fractures and the two-dimensional Rayleigh–Taylor instability. *J. Comput. Phys.*, 207, 2005, pp. 610-624.

Thoroddsen, S.T., Qian, B., Etoh, T.G. & Takehara, K. (2007). The initial coalescence of miscible drops. *Phys. Fluids,* 19, 2007, 1-21;

Wang, W., Gong, J., Ngan, K.H. & Angeli, P. (2009). Effect of glycerol on the binary coalescence of water drops in stagnant oil phase. *Chem. Eng. Res. Design,* 87, 2009, pp. 1640-1648;

Wu, M., Cubaud, T. & Ho, C. (2004). Scaling law in liquid drop coalescence driven by surface tension. *Phys. Fluids,* 16, 2004, pp. 51-54;

Xing, X.Q., Butler, D.L., Ng, S.H., Wang, Z., Danyluk, S. & Yang, C. (2007). Simulation of droplet formation and coalescence using lattice Boltzmann-based single-phase model. *J. Coll. Interf. Sci.*, 311, 2007, pp. 609-618;

Yiantsios, S.G. & Davis, R.H. (1991). Close approach and deformation of two viscous drops due to gravity and van der Waals forces. *J. Colloid Interface Sci.*, 144, 1991, pp. 412-433;

Yoon, Y., Baldessari, F., Ceniceros, H.D. & Leal, L.G. (2007). Coalescence of two equal-sized deformable drops in an axisymmetric flow. *Phys. Fluids*, 19, 2007, pp. 1-24;

Zhang, F.H., Li, E.Q. & Thoroddsen, S.T. (2009). Satellite formation during coalescence of unequal size drops. *Phys. Rev. Lett.*, 102, 2009, pp. 1-4;
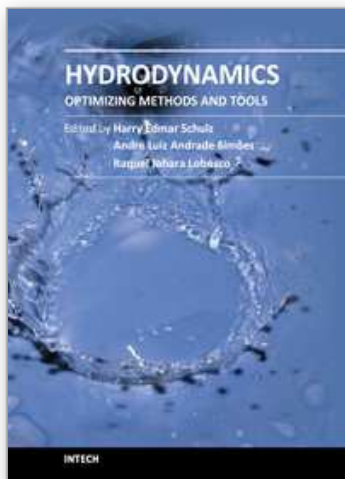
Hydrodynamics - Optimizing Methods and Tools
Edited by Prof. Harry Schulz

The constant evolution of the calculation capacity of the modern computers implies in a permanent effort to adjust the existing numerical codes, or to create new codes following new points of view, aiming to adequately simulate fluid flows and the related transport of physical properties. Additionally, the continuous improving of laboratory devices and equipment, which allow to record and measure fluid flows with a higher degree of details, induces to elaborate specific experiments, in order to shed light in unsolved aspects of the phenomena related to these flows. This volume presents conclusions about different aspects of calculated and observed flows, discussing the tools used in the analyses. It contains eighteen chapters, organized in four sections: 1) Smoothed Spheres, 2) Models and Codes in Fluid Dynamics, 3) Complex Hydraulic Engineering Applications, 4) Hydrodynamics and Heat/Mass Transfer. The chapters present results directed to the optimization of the methods and tools of Hydrodynamics.

How to reference
In order to correctly reference this scholarly work, feel free to copy and paste the following:

Alejandro Acevedo-Malavé and Máximo Garcîa-Sucre (2011). 3D Coalescence Collision of Liquid Drops Using Smoothed Particle Hydrodynamics, Hydrodynamics - Optimizing Methods and Tools, Prof. Harry Schulz (Ed.), ISBN: 978-953-307-712-3, InTech, Available from: http://www.intechopen.com/books/hydrodynamics-optimizing-methods-and-tools/3d-coalescence-collision-of-liquid-drops-using-smoothed-particle-hydrodynamics